Physics Letters B 797 (2019) 134835

Contents lists available at ScienceDirect

Physics Letters B

www.elsevier.com/locate/physletb

Isospin dependence of electromagnetic transition strengths among an isobaric triplet

A. Boso [a,c], S.A. Milne [b], M.A. Bentley [b,*], F. Recchia [a], S.M. Lenzi [a], D. Rudolph [d], M. Labiche [e], X. Pereira-Lopez [b], S. Afara [f], F. Ameil [g], T. Arici [g,h], S. Aydin [i], M. Axiotis [j], D. Barrientos [k], G. Benzoni [l], B. Birkenbach [m], A.J. Boston [o], H.C. Boston [o], P. Boutachkov [g], A. Bracco [l,p], A.M. Bruce [q], B. Bruyneel [r], B. Cederwall [s], E. Clement [t], M.L. Cortes [g,n], D.M. Cullen [u], P. Désesquelles [v], Zs. Dombràdi [w], C. Domingo-Pardo [x], J. Eberth [m], C. Fahlander [d], M. Gelain [j], V. González [y], P.R. John [a], J. Gerl [g], P. Golubev [d], M. Górska [g], A. Gottardo [z], T. Grahn [aa], L. Grassi [a], T. Habermann [g], L.J. Harkness-Brennan [o], T.W. Henry [b], H. Hess [m], I. Kojouharov [g], W. Korten [r], N. Lalović [d], M. Lettmann [n], C. Lizarazo [g], C. Louchart-Henning [g,n], R. Menegazzo [ab], D. Mengoni [a], E. Merchan [g], C. Michelagnoli [t], B. Million [l], V. Modamio [j], T. Moeller [n], D.R. Napoli [j], J. Nyberg [ac], B.S. Nara Singh [b,u], H. Pai [n], N. Pietralla [n], S. Pietri [g], Zs. Podolyak [ad], R.M. Perez Vidal [x], A. Pullia [p,l], D. Ralet [g,n,t], G. Rainovski [ae], M. Reese [g,n], P. Reiter [m], M.D. Salsac [r], E. Sanchis [y], L.G. Sarmiento [d], H. Schaffner [g], L.M. Scruton [b], P.P. Singh [g,af], C. Stahl [g,n], S. Uthayakumaar [b], J.J. Valiente-Dobón [j], O. Wieland [l]

[a] *Dipartimento di Fisica e Astronomia "Galileo Galilei", Università di Padova and INFN, Sezione di Padova, I-35131 Padova, Italy*
[b] *Department of Physics, University of York, Heslington, York, YO10 5DD, United Kingdom*
[c] *National Physical Laboratory, Hampton Road, Teddington, Middlesex TW11 0LW, United Kingdom*
[d] *Department of Physics, Lund University, S-22100 Lund, Sweden*
[e] *UKRI-STFC Daresbury Laboratory, Sci-Tech Daresbury, Daresbury, WA4 4AD, United Kingdom*
[f] *King Saud University, P. O. BOX 2454, Riyadh 11451, Saudi Arabia*
[g] *GSI Helmholtzzentrum für Schwerionenforschung, D-64291 Darmstadt, Germany*
[h] *Justus-Liebig-Universität Giessen, D-35392 Giessen, Germany*
[i] *Aksaray University, Bahçe Saray Mahallesi, Aksaray-Adana Yolu, 68100 Sağlık/Aksaray Merkez/Aksaray, Turkey*
[j] *INFN, Laboratori Nazionali di Legnaro, I-35020 Legnaro, Italy*
[k] *CERN, CH-1211 Geneva 23, Switzerland*
[l] *INFN Sezione di Milano, I-20133 Milano, Italy*
[m] *Institut für Kernphysik, Universität zu Köln, Zülpicher Str. 77, D-50937 Köln, Germany*
[n] *Institut für Kernphysik, Technische Universität Darmstadt, D-64289 Darmstadt, Germany*
[o] *Oliver Lodge Laboratory, The University of Liverpool, Liverpool, L69 7ZE, United Kingdom*
[p] *University of Milano, Dept. of Physics, I-20133 Milano, Italy*
[q] *School of Computing, Engineering and Mathematics, University of Brighton, Brighton BN2 4GJ, United Kingdom*
[r] *Irfu, CEA, Université Paris-Saclay, F-91191 Gif-sur-Yvette, France*
[s] *Department of Physics, Royal Institute of Technology, SE-10691 Stockholm, Sweden*
[t] *GANIL, Bd Henri Becquerel, BP 55027-14076 CAEN Cedex 05 France*
[u] *School of Physics and Astronomy, The University of Manchester, Oxford Rd, Manchester, M13 9PL, United Kingdom*
[v] *CSNSM, Université Paris-Sud and CNRS-IN2P3, Universié Paris-Saclay, Bat 104, F-91405 Orsay Campus, France*
[w] *Institute for Nuclear Research, Hungarian Academy of Sciences, ATOMKI, P.O.Box 51, H-4001 Debrecen, Hungary*
[x] *IFIC, CSIC-Universitat de Valencia, E-46980 Valencia, Spain*
[y] *Departamento de Ingeniería Electrónica, Universitat de Valencia, Burjassot, Valencia, Spain*
[z] *Institut de Physique Nucléaire, IN2P3-CNRS, Université Paris-Sud, Université Paris-Saclay, F-91405 Orsay, France*
[aa] *Department of Physics, University of Jyväskylä, FIN-40014, Finland*
[ab] *INFN Sezione di Padova, I-35131 Padova, Italy*
[ac] *Department of Physics and Astronomy, Uppsala University, SE-75120 Uppsala, Sweden*
[ad] *Department of Physics, University of Surrey, Guildford, GU2 7XH, United Kingdom*
[ae] *Faculty of Physics, St. Kliment Ohridski University of Sofia, 1164 Sofia, Bulgaria*

* Corresponding author.
E-mail address: michael.bentley@york.ac.uk (M.A. Bentley).

https://doi.org/10.1016/j.physletb.2019.134835

[af] Department of Physics, Indian Institute of Technology Ropar, Rupnagar - 140 001, Punjab, India

ARTICLE INFO

Article history:
Received 23 April 2019
Received in revised form 19 July 2019
Accepted 5 August 2019
Available online 13 August 2019
Editor: D.F. Geesaman

ABSTRACT

Electric quadrupole matrix elements, M_p, for the $J^\pi = 2^+ \rightarrow 0^+$, $\Delta T = 0$, $T = 1$ transitions across the $A = 46$ isobaric multiplet ^{46}Cr-^{46}V-^{46}Ti have been measured at GSI with the FRS-LYCCA-AGATA setup. This allows direct insight into the isospin purity of the states of interest by testing the linearity of M_p with respect to T_z. Pairs of nuclei in the $T = 1$ triplet were studied using identical reaction mechanisms in order to control systematic errors. The M_p values were obtained with two different methodologies: (i) a relativistic Coulomb excitation experiment was performed for ^{46}Cr and ^{46}Ti; (ii) a "stretched target" technique was adopted here, for the first time, for lifetime measurements in ^{46}V and ^{46}Ti. A constant value of M_p across the triplet has been observed. Shell-model calculations performed within the *fp* shell fail to reproduce this unexpected trend, pointing towards the need of a wider valence space. This result is confirmed by the good agreement with experimental data achieved with an interaction which allows excitations from the underlying *sd* shell. A test of the linearity rule for all published data on complete $T = 1$ isospin triplets is presented.

The exchange symmetry between the proton and the neutron is one of the most fundamental symmetries in modern physics, rooted in the near charge-symmetry and charge-independence of the nuclear force [1]. The concept led Heisenberg [2] to introduce the isospin quantum number (T) which can be assigned to any nuclear state such that, in the absence of charge-dependent forces, there will be an identical analogue state of the same isospin T in all isobars T_z ($= (N - Z)/2$) in the range $+T$ to $-T$.

In general, any interactions that depend on charge (the strongest of which is the electromagnetic interaction) are sufficiently weak that they do not disturb the symmetry of the underlying wave functions of these isobaric analogue states (IAS). Hence the assumption of identical wave functions among a set of IAS is usually considered to be safe. Much work has been undertaken recently studying differences in energy between excited states of mirror nuclei and $T = 1$ triplets (IAS with $T = 1$ in the three nuclei with $T_z = 0, \pm 1$) – see, for example, references [3–8]. In these analyses, symmetry of the underlying wave functions is assumed and so the differences in excitation energy were interpreted in terms of nuclear structure phenomena. In a shell-model analysis, it is found that additional isospin non-conserving interactions (INC), beyond the usual two-body Coulomb force, were required to account for the data, e.g. [3,6]. In the case of $T = 1$ triplets, the INC interactions required are consistently large, and it is speculated that the charge dependence of the nuclear interaction itself plays a significant role [9,10]. This analysis of INC forces, however, does not yield any information on the purity of the isospin quantum number or deviations from the presumed identicality of the analogue wavefunctions.

Isospin mixing can, however, be studied through testing predictions that **rely** on the isospin purity of a set of analogue states. The established method is the isobaric multiplet mass equation (IMME). The IMME predicts that the total binding energy in a multiplet should be a quadratic in T_z for a set of identical analogue states of pure isospin T in the presence of a two-body interaction with isoscalar, isovector and isotensor components. The IMME has been tested many times through high-precision mass measurements and, whilst there are a small number of notable deviations, the rule holds well – see, for example, Lam et al. [11] for a comprehensive review. Similar rules appear for electromagnetic transition strengths under the same assumptions as above for the IMME – see reference [12] for details. The isospin dependence of the proton matrix element for a set of $T \rightarrow T$ analogue electromagnetic transitions has a simple form, and for the analogue states of a $T = 1$ triplet may be written [13]

$$M_p(T_z) = \frac{1}{2}[M_0 - T_z M_1^{T_z=1}] \quad (1)$$

where M_0 and $M_1^{T_z=1}$ are the isoscalar matrix element and isovector matrix element (for the $T_z = 1$ nucleus) respectively. Thus, in the limit of pure isospin, the analogue proton matrix elements should be exactly linear with T_z. This rule is difficult to test precisely due to the experimental challenges in performing such measurements in proton-rich nuclei, since this requires either use of radioactive beams or production of nuclei from stable-beams but with very low cross sections. The most straightforward way to test this rule is through the study of a $T = 1$ triplet of nuclei and measurement of the analogue $B(E2)$ strengths between the $T = 1$, 0^+ ground state and the $T = 1$, 2^+ first excited state – in which case $B(E2)(T_z, 0^+ \rightarrow 2^+) = (M_p(T_z))^2$. Indeed, there is the potential for isospin mixing in the odd-odd $N = Z$ system due to the close proximity of the $T = 1$ and $T = 0$ states. Prados-Estevez et al. [14] performed a compilation of such $B(E2)$ strengths for all $T = 1$ triplets for $22 \leq A \leq 42$ and found, in general, good agreement with the rule within the error limits. There were some exceptions – most notably $A = 38$ [14] where deviation from linearity was indicated. However, for many of the cases shown, the error bars were too large to test linearity. Moreover, in general, the measurements for each triplet have come from different experiments, with different $B(E2)$ measurement methods and different population/feeding routes to the state of interest – hence hidden systematic errors cannot be ruled out.

The $A = 46$ triplet, the topic of this work, is the heaviest for which all three $B(E2)$s are known, although the errors in the $B(E2)$s for ^{46}Cr and ^{46}V (at 20% [15] and 13% [16] respectively) are too large to test for any non-linearity. The $A = 46$ triplet is especially interesting since systematics of the experimental $T = 0$ and $T = 1$ states in ^{46}V [18] indicate that the lowest $T = 1$ and $T = 0$ 2^+ states are likely to be very close in energy and hence may result in mixing of isospin. The aim of the work presented here was to address these issues by performing $B(E2)$ measurements for all three members of the $A = 46$ triplet. To reduce the impact of systematic errors, we also ensure that analogue $B(E2)$s are measured using the same technique, under identical experimental conditions, and that the states of interest were populated through an identical (analogue) mechanism. This enables a precise relative measurement of the transition strengths to test the

linearity rule. We also introduce here a method for lifetime measurements, especially suited to studies with fragmentation beams, which we call the "stretched target" technique.

The experiment was performed at the GSI Helmholtzzentrum für Schwerionenforschung, Germany, with the FRS-AGATA-LYCCA setup – see [19,20] for further details. A 600 MeV/A ^{58}Ni beam, provided by the SIS18 synchrotron, impinged on a 2.5 g/cm^2 Be primary target. The isotopes resulting from the fragmentation reaction were separated and identified with the double-stage magnetic spectrometer FRS [21] by means of the $B\rho - \Delta E - B\rho$ method, which allows precise determination of the atomic number Z and the mass over charge-state ratio, A/q. The energy loss of the ions was measured with two Multi Sample Ionisation Chambers (MUSICs) while the time of flight and the positions in the second and fourth focal planes were obtained from two plastic scintillators. Three different magnet settings were chosen to transmit the three secondary beams of interest, ^{46}Cr, ^{46}V and ^{46}Ti with beam energies of 180, 176 and 178 MeV/A respectively. The three beams impinged, separately, on two different secondary-target arrangements, described below, to measure the three analogue $0^+_{g.s.} \rightarrow 2^+_1$ $B(E2)$ strengths.

The secondary target (arrangement) was surrounded by the gamma ray tracking spectrometer AGATA [22], comprising, in this configuration, 22 HPGe detectors placed in the forward direction with respect to the beam line arranged in a combination of triple- and double-cryostats. For AGATA, the pulse-shape analysis methodology gives a position sensitivity of ≤ 5 mm which, in turn, is crucial for γ-ray photo-peak resolution, which would otherwise be destroyed by Doppler broadening effects at $\beta > 0.5$c, such as here. The outgoing ions were identified by the LYCCA calorimeter [23] which provides energy-loss, total energy and time-of-flight (ToF) measurements. The atomic number of the outgoing fragment was determined by E-ΔE measurement given by a combination of DSSSD and CsI detectors in the LYCCA "wall" [23]. Determination of the mass of the outgoing fragment was not necessary since the fragment of interest is the same as the incoming secondary beam in both cases. The two LYCCA plastic scintillators placed just before and 3.4 m after the secondary target provide a precise event-by-event ToF measurement which is essential for the event-by-event Doppler correction. A single DSSSD detector is placed in close proximity to the secondary target in order to determine the interaction position, and the complementary position information given by the wall DSSSDs therefore provides the track of the outgoing ions. The position information from the LYCCA detectors was coupled to this information to provide full reconstruction of the trajectory of the incoming and outgoing ions for the purpose of Doppler correction and determination of scattering angle.

Two different methods were employed to determine the $0^+_{g.s.} \rightarrow 2^+_1$ $B(E2)$ strengths. For each method two members of the triplet were measured – either ^{46}Cr/^{46}Ti or ^{46}V/^{46}Ti. Thus, in each case ^{46}Ti, for which the B(E2) is known very precisely, is measured, as a "reference" point to enable a relative measurement.

For the ^{46}Cr/^{46}Ti measurements, relativistic Coulomb excitation was used, for which the secondary-target comprised a 500 mg/cm^2 single gold foil. The cross section of the reaction is given by the relation:

$$\sigma_{\text{Coulex}} = \frac{N_\gamma}{N_B M_{TA}} \tag{2}$$

where N_B is the number of incoming ions detected in FRS, M_{TA} is the number of target atoms per unit area and N_γ is the number of counts in the γ-ray peak after background subtraction and efficiency corrections. In order to avoid any possible interference between the electromagnetic and the nuclear interactions, a cut on the scattering angle of the ion was applied, such that the minimum impact parameter is given by

$$b_{min} = r_0 \left(A_P^{1/3} + A_T^{1/3} \right) + 5 \text{ fm}$$

where $r_0 = 1.2$ fm. This resulted in an angle cut (maximum) of 20 mrad. The absolute AGATA efficiency was determined and corrected to take into account the effective number of working detectors, multiplicity effects, the Doppler boost due to the relativistic regime, dead-time contributions and the angular distribution of the transition. The final γ-ray spectra of ^{46}Ti and ^{46}Cr are reported in Fig. 1, in which the tracking capabilities of AGATA (γ-ray interaction position) and LYCCA (beam tracking and time of flight) have been used to perform event-by-event Doppler correction, resulting in a resolution of 12-14 keV.

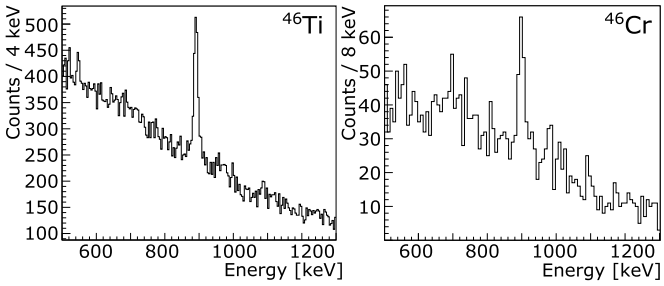

Fig. 1. Gamma-ray spectra for ^{46}Ti and ^{46}Cr produced using relativistic Coulomb excitation. Incoming and outgoing ions, time and scattering angle cuts are applied – see text for details.

Table 1
The measured $B(E2)^\uparrow$ $(0^+ \rightarrow 2^+)$ values obtained in this work from relativistic Coulomb excitation for ^{46}Ti and ^{46}Cr. The literature values are taken from references [16] and [15], respectively.

Setting	^{46}Ti	^{46}Cr
$B(E2)^\uparrow$ – This work [e^{2}fm^4]	918 ± 74	886 ± 158
$B(E2)^\uparrow$ – Literature [e^{2}fm^4]	965 ± 9	930 ± 200

The cross-section values obtained are (81.4 ± 6.6) mb for ^{46}Ti and (78.1 ± 14.0) mb for ^{46}Cr. The error budget is strongly dominated by the statistical contribution due to the number of counts in the γ-ray peaks. The electromagnetic transition probabilities have been obtained from the measured cross sections using the DWEIKO code [24], which provides calculations of elastic scattering differential cross sections, probabilities, and cross sections for inelastic scattering in nuclear collisions at intermediate and high energies in the framework of the Distorted Wave Born Approximation (DWBA), exploiting eikonal wave functions and solving coupled-channels equations [24]. The results are presented in Table 1 together with the previously reported values [15,16]. The ^{46}Ti result is consistent with the literature value, confirming the present analysis method. The ^{46}Cr measurement is also consistent with the literature value, with a slightly reduced error bar.

In the second method, for the ^{46}V/^{46}Ti measurements, lifetimes were determined using a new "stretched-target" method. A stack of three gold foils was used at the secondary target, to excite the ions of interest by electromagnetic interaction whilst measuring the lifetime using Doppler-shift effects. Each foil acts as both a target (to excite the 2^+_1 state through Coulomb excitation) and a degrader to vary the velocity of the incoming fragment. The result is a Doppler-shift profile that provides a distinctive line-shape with three peaks (for decays following the three targets), the shape of which depends on the lifetime. The target thicknesses were chosen to be $(750 + 500 + 500)$ mg/cm^2, separated by two 1 mm gaps, all of which was optimised to provide maximum sensitivity

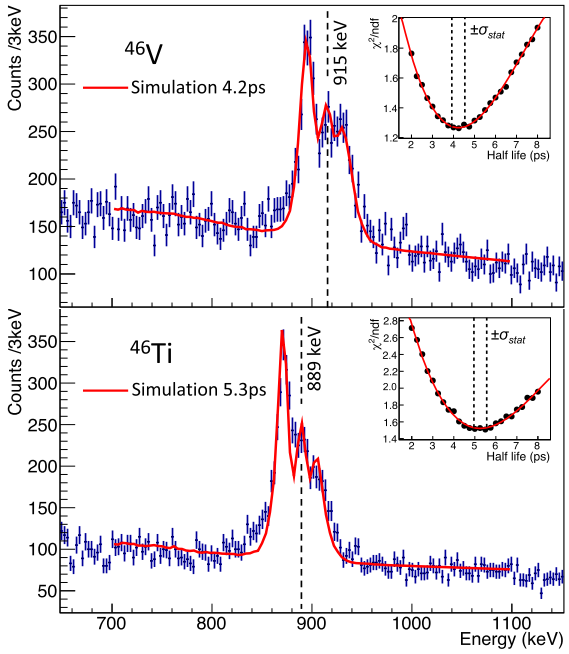

Fig. 2. Gamma-ray spectra for ^{46}V (top) and ^{46}Ti (bottom) using the triple-gold-foil "stretched-target" method. The Doppler correction has been optimised for the central "peak", and the correct energy of the transition is marked by the dashed line. Only AGATA detectors at an angle $\leq 50°$ to the beam direction are included, and an angle-dependent correction has been applied to spectrum to ensure that the peak centroids are at the same location for all angles. The solid (red) line is a full AGATA simulation produced under the same conditions as the experiment – see text for details. Inset: The χ^2 values (per degree of freedom) as a function of half life, and the resulting polynomial fit used to determine the half life and the statistical errors, also shown – see text for details.

to half lives in the 5 ps region. The three average velocities after the targets were, for ^{46}Ti (for example), $v/c = 0.527$, 0.509 and 0.488 respectively for decays after each of the three foils in turn. In this analysis, the Doppler correction was performed for the central "peak" which means that the position of the two other peak centroids will be dependent on angle. Since AGATA provides event-by-event angle information, a correction was applied to move the peak centroids to the same location in the spectrum for all angles. In this way the full range of angles can be included in a single spectral analysis for the lifetime. Events for all available laboratory angles $\leq 50°$ were included (see below). The resulting spectra are shown in Fig. 2. In these spectra, and in the Coulomb excitation spectra in Fig. 1, the $2^+_1 \rightarrow 0^+_{g.s.}$ transition is the only peak observed in the whole spectrum.

In order to determine the lifetime, a full simulation was produced of the γ-ray spectral response. This involved a GEANT4 [25] simulation using an event generator that allows for Coulomb excitation of the single state (2^+_1) in each of the three targets. The secondary beam parameters (velocity, momentum spread, spatial distribution) were simulated from well-established ion-optical transport codes, and adjusted to match the observed experimental conditions. The γ-ray response was simulated through coupling this event generator to the full AGATA simulation code [26]. The experimental spectral resolution is dominated by the particle tracking capability of the system, specifically the effective LYCCA ToF resolution, which was adjusted in the simulation to reproduce the experimental width from the single-target spectra. The simulated data were then passed through the same analysis procedure as the experimental data. The final simulated spectrum was produced by adding the lineshape from the target to a polynomial background, the parameters of which were extracted from a fit

Table 2
The measured half-life values obtained in this work from the stretched-target method for ^{46}Ti and ^{46}V. The literature values are both taken from reference [16]. The corresponding experimental $B(E2)^{\uparrow}$ ($0^+ \rightarrow 2^+$) values are shown.

	^{46}Ti	^{46}V
$T_{1/2,exp}$ [ps]	5.26(34)	4.23(35)
$T_{1/2,lit}$ [ps]	5.29(5) [16]	4.7(6) [16]
$B(E2)^{\uparrow}$ [e^{2}fm^4]	970(63)	1044(86)

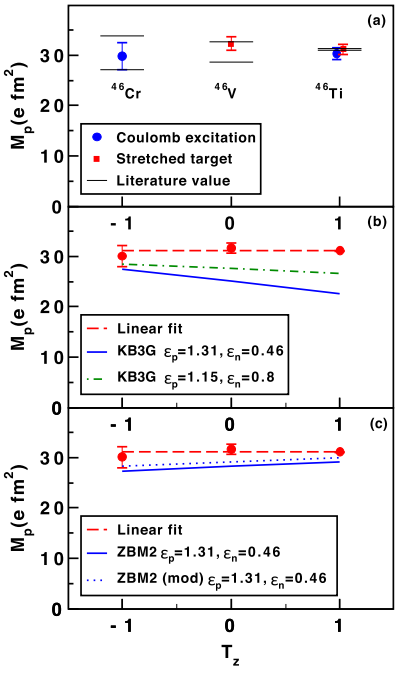

Fig. 3. (a): Absolute values of the transition matrix elements M_p determined from the present work. The solid lines indicate the error limits of the current literature values [15,16]. (b): (Data) The weighted average values of M_p for all published data combined with the present work. The red dashed line is a linear fit to the data. Shell-model calculations using the KB3G interaction are shown by the solid and dot-dashed lines. (c): Data as (b). Shell-model calculations using the ZBM2 interaction are shown by the solid line. The dotted line (mod) shows the result of the shell model calculation if the $p_{3/2}$ level is lowered by 500 keV.

to the experimental spectrum between 700 and 1100 keV. For a specific simulated lifetime, the background and lineshape intensity were allowed to vary freely to obtain the best fit. This procedure was repeated, varying both the half life and the upper angle cut, to create a χ^2 surface. This was used to determine the optimum upper angle cut (i.e. narrowest χ^2 on the half-life axis). This yielded the upper angle cut of 50° which was used for both ^{46}V and ^{46}Ti. The half life was determined from a fit of the resulting $T_{1/2}$ vs χ^2 plot and the statistical error determined from the evaluation of that fit at $\chi^2_{min} + 1$. The analysis yields 4.23(31) and 5.26(30) ps (statistical errors) for ^{46}V and ^{46}Ti respectively. A systematic error was determined by varying, in the simulation, the two effects expected to have the strongest effect on the lineshape – the small energy dependence of the cross-section through the targets (calculated using DWEIKO for the simulation) and the gaps between the foils. For the former we introduced a 15% variation in the energy dependence and for the latter we allowed all three foils to move by ±100 μm. This yielded a 0.17 ps systematic error which was added in quadrature. The final results, and the corresponding $0^+_{g.s.} \rightarrow 2^+_1$ $B(E2)$ strengths are quoted in Table 2. Again, the agreement with the literature values is good, with the value for ^{46}V having a much reduced error bar.

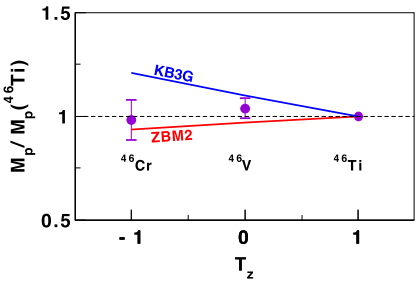

Fig. 4. The measured proton matrix elements M_p from this work for ^{46}Cr and ^{46}V, plotted relative to the measured value for ^{46}Ti (from this work) for the Coulomb excitation (Cr/Ti) and stretched target (V/Ti) data. The shell model calculations plotted correspond to the solid lines in Figs. 3(a) and (b).

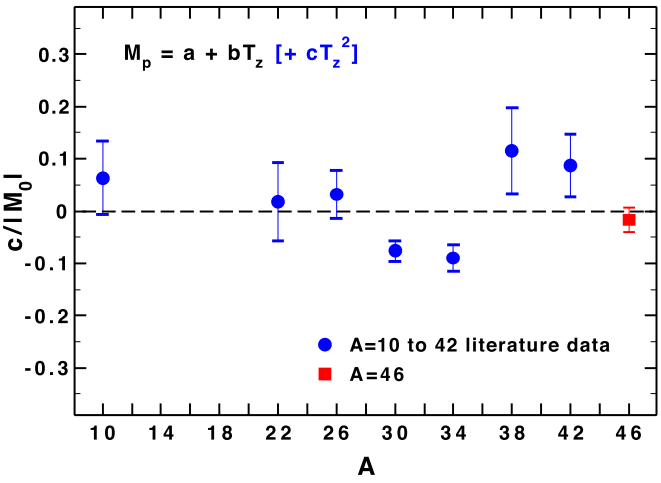

Fig. 5. The c coefficients from the expression $M_p = a + bT_z + cT_z^2$ extracted from a fit to all published experimental data for $T = 1$ triplets for $A \leq 42$ (circles) and the new values for $A = 46$ (square). Data are taken from [27–30] for the $T_z = \pm 1$ nuclei and [31–37] for the $T_z = 0$ nuclei. The c coefficients are plotted relative to the experimental isoscalar matrix element M_0 – see text for details.

The absolute values of the proton transition matrix elements determined in this work are plotted in Fig. 3(a). The good agreement with the literature values for ^{46}Ti validates both methods. Since the aim was to determine relative B(E2)s across the triplet, the measured ratios M_p(Cr)/M_p(Ti) (from Coulex) and M_p(V)/M_p(Ti) (stretched target) are shown in Fig. 4. Since the conditions were identical for each measurement, only statistical errors have been included for the relative measurements. To reduce the error bars further, the values obtained in this work have been combined with the data from references [15–17] in a weighted average, and shown in Figs. 3(b) and (c), along with a linear fit (dashed line). It is clear that the isospin rule (linearity of the matrix element with T_z) holds extremely well – implying no evidence for isospin mixing. Indeed, the M_p values are remarkably constant across the triplet. This, in turn, implies a vanishingly small isovector proton matrix element – the linear fit (see Eq. (1)) yielding 0.0(15) and 62.2(15) efm^2 for the isovector and isoscalar matrix elements respectively. A recent complication of all available data by Morse et al. [42] indicates that measured isovector matrix elements are consistently small, relative to the isoscalar.

The linearity rule for transition matrix elements can be tested, generally, for isospin multiplets, by fitting a quadratic expression of the form $M_p = a + bT_z + cT_z^2$ and extracting the c coefficient – which should be zero in the limit of exact isospin symmetry. We have performed this analysis for the eight complete $T = 1$ triplets that exist in the literature, and the results are plotted in Fig. 5. The data (i.e. M_p) for the even-even members of the $A = 10 - 42$ triplets are taken from the recent compilation of $B(E2)$s [27], with more recent published results [28–30] included through adding them as a weighted average. Data for the odd-odd members of the triplet are taken from the most recent evaluations [31–36] and recent results on ^{10}B [37]. The data used for $A = 46$ are the weighted averages plotted in Fig. 3(b). Since the total matrix element varies significantly in this mass range, we have plotted the extracted c-coefficients normalised to the isoscalar matrix element, M_0 (extracted from a linear fit to the same data – see Eq. (1)). As expected the $A = 46$ triplet c-coefficient is consistent with zero, and it is clear that the $A = 46$ data now provide one of the most precise tests of the rule to date. It can also be seen that data on $A = 30, 34$ now deviate significantly from the prediction, once the most recent data are included.

The near equality of the experimental values for M_p for $A = 46$ is, intuitively, unexpected since, assuming an inert ^{40}Ca core, the larger atomic number of ^{46}Cr should induce a higher transition probability. These data have been compared with shell-model calculations using the KB3G interaction [38] in the fp valence space, as shown in Fig. 3(b). Calculations using the effective charges of reference [39], usually considered to be appropriate for this region, are shown by the solid line in Fig. 3(b) and the upper line in Fig. 4. The data are not well reproduced, neither in magnitude nor T_z-dependence. Du Reitz et al. [40] derived a set of effective charges from the $A = 51$ mirror nuclei, through determination, separately, of the isoscalar and isovector polarisation charges. The effective charges in this case were closer for protons and neutrons ($\varepsilon_p = 1.15, \varepsilon_n = 0.8$). Indeed, the application of these charges here results in a flatter dependence of M_p with T_z (see dotted line in Fig. 3(b)). The overall agreement, however, remains poor.

The above analysis clearly points towards the inadequacy of the fp valence space for these nuclei, suggesting the importance of core excitations from the underlying sd shell. To overcome this issue we used the ZBM2 interaction [41], with an inert core of ^{28}Si and the valence space consisting of the $s_{1/2} - d_{3/2} - f_{7/2} - p_{3/2}$ orbits. This is shown by the solid line in Fig. 3(c) and the lower line in Fig. 4, where the effective charges of [39] are used as before. Now the magnitude and T_z-dependence are much better reproduced. This clearly indicates that, for the $A = 46$ nuclei, the ^{40}Ca core is not closed, and the only way to explain the very flat dependence of the matrix elements with T_z is by having a much larger (and hence more similar across the triplet) number of valence protons active for the 2_1^+ state through particle-hole excitations. This is consistent with the fact that the $A = 46$ mirror energy differences are unusually poorly reproduced by a shell-model analysis involving only the fp valences space – see, for example, reference [3]. The ZBM2 calculations (solid line in Fig. 3(c)) still do not reproduce the full magnitude of the $B(E2)$. This is likely due to the lack of the $f_{5/2}$, $p_{1/2}$ and $d_{5/2}$ orbitals. Since quadrupole excitations are mainly due to the coupling of $\Delta L = 2$ orbits, their absence will affect the $B(E2)$. To demonstrate this, the energy gap between the $f_{7/2}$ and the $p_{3/2}$ orbits was artificially reduced by 500 keV, to increase the $\Delta L = 2$ interactions between the fp orbits. Indeed the agreement is now within error for two members of the triplet – see the dotted line in Fig. 3(c)).

In conclusion, the rule that (in the limit of pure isospin) the electromagnetic matrix elements should be exactly linear with T_z has been tested with high precision for the heaviest $T = 1$ triplet for which data are currently available in the literature. We have compared our results with an analysis of the linearity rule for all known $T = 1$ triplets. An experimental method has been used that allows for a reliable *relative* measurement through using the same technique, experimental conditions and analogue population mechanism for different members of the triplet – hence reducing the impact of any systematic errors. The experiment was

performed with the AGATA array where the superb position sensitivity and tracking capability of the new LYCCA set-up allowed for a high-resolution analysis. We have introduced a new method for lifetime analysis, the stretched target method, made possible by this high resolution. This method is especially well suited to spectroscopy using exotic fragmentation beams of high velocity ($\beta \geq 0.5$), and so would be ideal for AGATA experiments at the future FAIR facility.

Acknowledgements

This work was supported by the UK Science and Technology Facilities Council (STFC) under Grant Nos. ST/L005727, ST/G000670, ST/J000124 and ST/P003885, the European Commission FP7-Capacities, ENSAR Contract No. 262010, the Swedish Research Council under Contracts Nos. 2010-147, 2011-5253 and 2011-6127, BMBF NuSTAR-AGATA 05P15RDFN9 and BMBF NuSTAR 05P15RDFN1.

References

[1] R. Machleidt, I. Slaus, J. Phys. G, Nucl. Part. Phys. 27 (2001) R69–R108.
[2] W. Heisenberg, Z. Phys. 77 (1932) 1.
[3] M.A. Bentley, S.M. Lenzi, Prog. Part. Nucl. Phys. 59 (2007) 497.
[4] J. Ekman, C. Fahlander, D. Rudolph, Mod. Phys. Lett. A 20 (2005) 2977.
[5] S.M. Lenzi, M.A. Bentley, R. Lau, C.Aa. Diget, Phys. Rev. C 98 (2018) 054322.
[6] M.A. Bentley, S.M. Lenzi, S.A. Simpson, C.Aa. Diget, Phys. Rev. C 92 (2015) 024310.
[7] S.A. Milne, et al., Phys. Rev. Lett. 117 (2016) 082502.
[8] A. Boso, et al., Phys. Rev. Lett. 121 (2018) 032502.
[9] A. Gadea, et al., Phys. Rev. Lett. 97 (2006) 152501.
[10] W.E. Ormand, B.A. Brown, M. Hjorth-Jensen, Phys. Rev. C 96 (2017) 024323.
[11] Y.H. Lam, N.A. Smirnova, E. Caurier, Phys. Rev. C 87 (2013) 054304.
[12] E.K. Warburton, J. Weneser, in: D.H. Wilkinson (Ed.), Isospin in Nuclear Physics, North-Holland, Amsterdam, 1969, Chap. 5.
[13] A.M. Bernstein, V.R. Brown, V.A. Madsen, Phys. Rev. Lett. 42 (1979) 425.
[14] F.M. Prados Estevez, et al., Phys. Rev. C 75 (2007) 014309.
[15] K. Yamada, et al., Eur. Phys. J. A 25 (2005) 409.
[16] O. Möller, et al., Phys. Rev. C 67 (2003) 011301.
[17] F. Brandolii, et al., Phys. Rev. C 64 (2001) 044307.
[18] S.M. Lenzi, et al., Phys. Rev. C 60 (1999) 021303.
[19] N. Lalović, et al., Nucl. Instrum. Methods A 806 (2016) 258.
[20] D. Ralet, et al., Phys. Rev. C 95 (2017) 034320.
[21] H. Geissel, et al., Nucl. Instrum. Methods B 70 (1992) 286.
[22] S. Akkoyun, et al., Nucl. Instrum. Methods A 668 (2012) 26.
[23] P. Golubev, et al., Nucl. Instrum. Methods A 723 (2013) 55.
[24] C.A. Bertulani, T. Glasmacher, C.M. Campbell, Comput. Phys. Commun. 152 (2003) 317.
[25] J. Allison, et al., Nucl. Instrum. Methods A 835 (2016) 186.
[26] E. Farnea, et al., Nucl. Instrum. Methods A 621 (2010) 331.
[27] B. Pritychenko, M. Birch, B. Singh, M. Horoi, At. Data Nucl. Data Tables 107 (2016) 1–139.
[28] J. Henderson, et al., Phys. Lett. B 782 (2018) 468–473.
[29] P. Petkov, et al., Phys. Rev. C 96 (2017) 034326.
[30] K. Hadynska-Klek, et al., Phys. Rev. Lett. 117 (2016) 062501.
[31] M.S. Basunia, Nucl. Data Sheets 127 (2015) 69–190.
[32] M.S. Basunia, A.M. Hurst, Nucl. Data Sheets 134 (2016) 1–148.
[33] M.S. Basunia, Nucl. Data Sheets 111 (2010) 2331–2424.
[34] N. Nica, B. Singh, Nucl. Data Sheets 113 (2012) 1563–1733.
[35] J. Chen, Nucl. Data Sheets 152 (2018) 1–130.
[36] J. Chen, B. Singh, Nucl. Data Sheets 135 (2016) 1–192.
[37] S. Kuvin, et al., Phys. Rev. C 96 (2017) 041301(R).
[38] A. Poves, J. Sanchez-Solano, E. Caurier, F. Nowacki, Nucl. Phys. A 694 (2001) 157.
[39] M. Dufour, A.P. Zuker, Phys. Rev. C 54 (1996) 1641.
[40] R. du Rietz, et al., Phys. Rev. Lett. 93 (2004) 222501.
[41] E. Caurier, K. Langanke, G. Martínez-Pinedo, F. Nowacki, P. Vogel, Phys. Lett. B 522 (2001) 240.
[42] C. Morse, et al., Phys. Lett. B 787 (2018) 198–203.